Journal of Computational Physics 229 (2010) 7440–7455

Contents lists available at ScienceDirect

Journal of Computational Physics

journal homepage: www.elsevier.com/locate/jcp

A level set method for the semiclassical limit of the Schrödinger equation with discontinuous potentials

Dongming Wei [a,*], Shi Jin [a], Richard Tsai [b], Xu Yang [c]

[a] Department of Mathematics, University of Wisconsin, Madison, WI 53706, USA
[b] Department of Mathematics, University of Texas at Austin, Austin, TX 78712, USA
[c] Program in Applied and Computational Mathematics, Princeton University, Princeton, NJ 08544, USA

ARTICLE INFO

Article history:
Received 20 January 2010
Received in revised form 13 May 2010
Accepted 14 June 2010
Available online 23 June 2010

Keywords:
Schrödinger equation
Level set
Interface

ABSTRACT

We propose a level set method for the semiclassical limit of the Schrödinger equation with discontinuous potentials. The discontinuities in the potential corresponds to potential barriers, at which incoming waves can be partially transmitted and reflected. Previously such a problem was handled by Jin and Wen using the Liouville equation – which arises as the semiclassical limit of the Schrödinger equation – with an interface condition to account for partial transmissions and reflections (S. Jin, X. Wen, SIAM J. Num. Anal. 44 (2006) 1801–1828). However, the initial data are Dirac-delta functions which are difficult to approximate numerically with a high accuracy. In this paper, we extend the level set method introduced in (S. Jin, H. Liu, S. Osher, R. Tsai, J. Comp. Phys. 210 (2005) 497–518) for this problem. Instead of directly discretizing the Delta functions, our proposed method decomposes the initial data into finite sums of smooth functions that remain smooth in finite time along the phase flow, and hence can be solved much more easily using conventional high order discretization schemes.

Two ideas are introduced here: (1) The solutions of the problems involving partial transmissions and partial reflections are decomposed into a finite sum of solutions solving problems involving only complete transmissions and those involving only complete reflections. For problems involving only complete transmission or complete reflection, the method of JLOT applies and is used in our simulations; (2) A reinitialization technique is introduced so that waves coming from multiple transmissions and reflections can be combined seamlessly as new initial value problems. This is implemented by rewriting the sum of several delta functions as one delta function with a suitable weight, which can be easily implemented numerically. We carry out numerical experiments in both one and two space dimensions to verify this new algorithm.

1. Introduction

In this paper, we propose a numerical scheme for the Liouville equation

$$f_t + H_\xi \cdot \nabla_{\mathbf{x}} f - H_{\mathbf{x}} \cdot \nabla_\xi f = 0, \quad t > 0, \quad \mathbf{x},\ \xi \in \mathbb{R}^d, \tag{1.1}$$

whose solutions are delta functions of variable weight concentrating on the bi-characteristics strips of the equation. The function $f(t,\mathbf{x},\xi)$ is the density distribution of particles depending on position $\mathbf{x}$, time t and velocity ξ. The Hamiltonian H takes the form

* Corresponding author. Tel.: +1 608 263 5686; fax: +1 608 263 8891.
E-mail addresses: dwei@math.wisc.edu (D. Wei), jin@math.wisc.edu (S. Jin), ytsai@math.utexas.edu (R. Tsai), xuyang@math.princeton.edu (X. Yang).

0021-9991/$ - see front matter © 2010 Elsevier Inc. All rights reserved.
doi:10.1016/j.jcp.2010.06.026

$$H(\mathbf{x},\xi)=\frac{1}{2}|\xi|^2+V(\mathbf{x}), \tag{1.2}$$

with $V(\mathbf{x})$ corresponding to the potential function. In particular, we are concerned with the case when the potential $V(\mathbf{x})\in W^{1,1}$ has jump discontinuities along a smooth hypersurface; such type of potentials correspond physically to problems with potential barriers.

Eq. (1.1) provides a phase space description of the semiclassical limit [6,20] of the Schödinger equation:

$$i\hbar\partial_t\psi^\hbar=-\frac{\hbar^2}{2}\Delta\psi^\hbar+V(\mathbf{x})\psi^\hbar,\quad \mathbf{x}\in\mathbb{R}^d, \tag{1.3}$$

where $\psi^\hbar$ is the complex-valued wave function, $\hbar$ the reduced Planck constant. In this setting, one typically considers the Schrödinger equation (1.3) with the WKB initial data assuming the form

$$\psi(\mathbf{x},0)=A_0(\mathbf{x})\exp(iS_0(\mathbf{x})/\hbar), \tag{1.4}$$

with smooth S_0. In the semiclassical limit $\hbar\to 0$, this corresponds to mono-kinetic initial data for the Liouville equation (1.1):

$$f(0,\mathbf{x},\xi)=|A_0(\mathbf{x})|^2\delta(\xi-\nabla_{\mathbf{x}}S_0(\mathbf{x})). \tag{1.5}$$

Consequently, the solutions of the initial value problem (1.1) and (1.5) remain as delta functions concentrating on the bi-characteristics.

When potential barriers are present in the problem, the potential function V has jump discontinuities along the barrier. Waves traveling into a potential barrier typically undergo partial transmissions and reflections; i.e. a proportion of an incident wave is transmitted through the discontinuity of the potential while the remaining portion is reflected. [1,21,25]. In this paper, we shall use the terms complete transmission or complete reflection when each incident ray is either transmitted through or reflected off the interface, and we shall refer to the discontinuities in the potential function as the interface.

It is possible to solve the Liouville equation (1.1) with delta function initial data (1.5) by replacing the initial data with approximate delta functions. We shall refer to this type of methods as the *direct methods*. However, this type of methods usually produces poor quality approximations as the delta functions are quickly smeared out due to numerical dissipation, and that the large gradient of the numerical approximations of the delta functions result in very large error constants.

To avoid computing directly the delta function solutions, one can track the bi-characteristic strips of the Liouville equation either explicitly [5] or implicitly [23,3,13,9,24,19], and evolve various physical quantities defined on the bi-characteristics along the way. In the context of solving the Schrödinger equation, the method introduced in [9] decomposes the particle density function f into ψ and ϕ_j ($j=1,\ldots,d$):

$$f(\mathbf{x},\xi,t)=\psi(\mathbf{x},\xi,t)\Pi_{j=1}^d\delta(\phi_j(\mathbf{x},\xi,t)), \tag{1.6}$$

where ψ and ϕ_j solve the same Liouville equation (1.1) with initial data

$$\psi(\mathbf{x},\xi,0)=\rho_0(\mathbf{x}),\quad \phi_j(\mathbf{x},\xi,0)=(\xi-\mathbf{u}_0(\mathbf{x}))_j, \tag{1.7}$$

respectively. Here $(\xi-\mathbf{u}_0(\mathbf{x}))_j$ denotes the jth component of the vector. In this setup, the common zeros of ϕ_j defines the bi-characteristics and ψ tracks the density on the bi-characteristics. We shall refer to such methods as *decomposition methods*.

The decomposition methods allow for numerical computations of bounded solutions rather than the measure-valued solution of the Liouville equation with singular initial data (1.5). Physical observables of the system (such as the density ρ and momentum $\rho\mathbf{u}$) can be computed passively via simple integrals in the phase dimensions

$$\rho(\mathbf{x},t)=\int\psi(\mathbf{x},\xi,t)\Pi_{i=1}^d\delta(\phi_i)d\xi, \tag{1.8}$$

$$\mathbf{u}(\mathbf{x},t)=\int\psi(\mathbf{x},\xi,t)\xi\Pi_{i=1}^d\delta(\phi_i)d\xi/\rho(\mathbf{x},t). \tag{1.9}$$

For problems involving complete transmissions and reflections, interface conditions can be formulated to capture such phenomena. The level set method proposed in [2] uses such idea to capture the reflections of wave fronts for the wave equations. It was also mentioned in [23] that an interface condition is needed to incorporate Snell's Law of Refraction into the transmission of wave fronts. In [14,15] a transmission and reflection interface condition was introduced for the Liouville equation (1.1) and a corresponding Hamiltonian preserving scheme was developed for complete transmissions and reflections for problems containing potential barriers or discontinuous wave speeds. Then the decomposition method of [9] was used to offer a more accurate numerical approximation. However, when one has to deal with *partial* transmissions and reflections using such an interface condition, as was done in [16] (and subsequent extensions to quantum barriers [10–12] and wave diffractions [17,18]), the direct method still works while the decomposition method requires additional level set functions to be added each time a ray in the incoming wave splits into a reflected one and a transmitted one [16]. This can be easily understood from the Lagrangian point of view. For smooth potentials V the solution to the Liouville equation (1.1) can be defined by the method of characteristics defined by the Hamiltonian system

$$\frac{\partial \mathbf{x}}{\partial t} = \nabla_{\xi} H, \quad \frac{\partial \boldsymbol{\xi}}{\partial t} = -\nabla_{\mathbf{x}} H. \tag{1.10}$$

However, at discontinuity of V, in order to define a physically relevant solution to the initial value problem of (1.10), a particle (or a characteristic defined by (1.10)) is split into two particles with weights corresponding to the transmission and reflection coefficients [11,7]. Since each level set Liouville equation (1.1) is the phase representation of the particle trajectory determined by (1.10), when a particle splits at the interface, one has to add another level set function to describe such a particle or ray splitting. With multiple partial transmissions and reflections, the total number of level set functions will increase exponentially in time [16].

In this paper, we extend the decomposition method so that partial transmissions and reflections that occur in the problems with potential barriers can be captured with a fixed number of level set functions, independent of how many times partial transmissions and reflections occurs at points on the interface. In order to achieve this, we introduce two new ideas. First, we decompose the problem with *partial* transmission and reflection into the sum of problems with only *complete* transmissions and reflections, so the decomposition method of Jin–Liu–Osher–Tsai can be used here as in [14,15].

Since this decomposition is valid only if the waves or particles hit the interface at most once, we need to utilize a reinitialization technique, which is the second new idea of the paper. After particle transmissions and reflections f no longer has the form of (1.6). Rather it is a superposition of several functions of the form (1.6). In order to continue to use the decomposition, we need to rewrite f in the form of (3.8). A simple numerical procedure is introduced for this purpose. This enables us to handle multiple transmissions and reflections for a long time.

Details of the decomposition is presented in Section 2. The level set algorithm for the decomposition method is presented in Section 3; this is followed by details about the reinitialization step in Section 4. In Section 5, we present some examples computed using the proposed numerical methods. The paper is concluded in Section 6.

2. Decomposition of the interface problem

Consider a point $\mathbf{x}$ on the interface. Since the interface is a hypersurface in the physical domain, we may consider the "left" and the "right" side of the interface at this point. Denote it by $\mathbf{x}^-$ and $\mathbf{x}^+$. The transmission-reflection interface condition for the Liouville equation (1.1) at $(\mathbf{x}^+, \xi)$, for phase directions pointing *into* the "right" of the interface, can be written in a general form as

$$f(t, \mathbf{x}^+, \xi) = \alpha_T f(t, \mathbf{x}^-, \xi_T) + \alpha_R f(t, \mathbf{x}^+, \xi_R), \tag{2.1}$$

where ξ_T and ξ_R are two functions depending on the interface normal at $\mathbf{x}$ and the phase variable ξ; α_T and α_R are transmission and reflection coefficients that may depend on ξ_T and ξ_R. This boundary condition dictates that the the density of particles at $(\mathbf{x}^+, \xi)$ are the sum of what is being transmitted, $f(t, \mathbf{x}^-, \xi_T)$, and what is being reflected $f(t, \mathbf{x}^+, \xi_R)$ from appropriate phases and sides of the interface.

Since the Liouville equations and the Schrödinger equation are translation and rotation invariant, we may assume that a point of interest on the interface is at the origin of the spatial domain and the x-axis is parallel to the normal of the interface at least locally. Thus, without loss of generality, we discuss the decomposition idea in the following model problem in two dimensions (one in space and one in phase). Thus, we assume that the interface is at $x = 0$ and the potential takes on the values V^+ and V^- from the right and the left, respectively. At $(0^+, \xi)$, $\xi > 0$, the transmission comes from the left side of the interface with a phase gradient which has the same sign as ξ and satisfies the condition for the conservation of Hamiltonian:

$$\frac{1}{2}\xi^2 + V^+ = \frac{1}{2}\xi_T^2 + V^-, \quad \xi_T > 0. \tag{2.2}$$

The reflection comes from the same side of the interface as 0^+ with a phase gradient which has the opposite sign from ξ and satisfies

$$\frac{1}{2}\xi^2 + V^+ = \frac{1}{2}\xi_R^2 + V^+, \quad \xi_R < 0. \tag{2.3}$$

To simplify the notation, we introduce two new notations, ξ^+ and ξ^-, where ξ^+ and ξ^- have the same sign and they satisfy the relationship

$$\frac{1}{2}(\xi^+)^2 + V^+ = \frac{1}{2}(\xi^-)^2 + V^-. \tag{2.4}$$

Then at $(0^+, \xi^+)$, $\xi^+ > 0$, (2.2) and (2.3) can be rewritten as $\xi_T = \xi^-$ and $\xi_R = -\xi^+$. Similarly, one can derive the condition for $(0^-, \xi^-)$, $\xi^- \leqslant 0$. Combining the two possible cases of 0^- and 0^+, we have

$$\begin{cases} \partial_t f + \xi f_x - V_x f_\xi = 0, \quad t > 0, \ x \neq 0, \\ f(0, x, \xi) = f_0(x, \xi), \\ f(t, 0^+, \xi^+) = \alpha_R(\xi^+) f(t, 0^+, -\xi^+) + \alpha_T(\xi^-) f(t, 0^-, \xi^-), \quad \xi^+ \geqslant 0, \\ f(t, 0^-, \xi^-) = \alpha_R(\xi^-) f(t, 0^-, -\xi^-) + \alpha_T(\xi^+) f(t, 0^+, \xi^+), \quad \xi^- \leqslant 0. \end{cases} \tag{2.5}$$

ξ^+ and ξ^-, having the same sign, satisfy the conservation of Hamiltonian

$$\frac{1}{2}(\xi^-)^2 + V^- = \frac{1}{2}(\xi^+)^2 + V^+. \tag{2.6}$$

The well-posedness of (2.5) was shown in [16].

For now, we assume that the characteristics of the Liouville equation, defined by (1.10), emanating from the support of $f_0(x,\xi)$ at time 0, intersect the interface at most once in the interval $[0,\tau_1]$ for some $\tau_1 > 0$. Let $\Omega(\tau)$ denote all (x,ξ) such that they can be traced backward from time τ to time 0 along the characteristics of the Liouville equation without intersecting with the interface $x = 0$. We can then easily write down the solution for (2.5) as follows:

- If $(x,\xi) \in \Omega(\tau)$, then
$$f(\tau,x,\xi) = f_0(x_0,\xi_0); \tag{2.7}$$
here (x,ξ) and (x_0,ξ_0) are respectively the coordinates of the unique characteristics at time τ and at time 0.
- If $(x,\xi) \in \Omega^c$, then
$$f(\tau,x,\xi) = \alpha_R(\xi^+)f(t_c,0^+,-\xi^+) + \alpha_T(\xi^-)f(t_c,0^-,\xi^-) = \alpha_R(\xi^+)f_0(x_0^R,\xi_0^R) + \alpha_T(\xi^-)f_0(x_0^T,\xi_0^T). \tag{2.8}$$
Here t_c is the time at which the characteristics emanating from (x_0^R,ξ_0^R) and from (x_0^T,ξ_0^T) at time 0 arrive at the interface $x = 0$. From this time on, these two rays travels along the same path and arrive at (x,ξ) at time τ. See Fig. 1.

The solution at points lying in the left side of the interface, i.e. (x,ξ): $x \leqslant 0$, is a sum of values that are convected along the characteristics that came from the same side and remain in the same side, maybe due to reflection, and those that were transmitted from the other side.

Hence, the density function f can be decomposed into the sum of the solutions of three interface problems of the same Liouville equation, but with only either *complete* transmissions or reflection. This fact is summarized in the following theorem. We shall refer to such solutions as the generalized characteristics solutions.

Theorem 2.1. *Let f be the generalized characteristic solution of (2.5). Define $\mathcal{L}f := \partial_1 f + \xi f_x - V_x f_\xi$, and consider the following three initial value problems with interface conditions:*

$$\begin{cases} \mathcal{L}f^R = 0, \quad f^R(0,x,\xi) = f_0^R(x,\xi) := f_0(x,\xi), \\ f^R(t,0^+,\xi^+) = \alpha_R(\xi^+)f^R(t,0^+,-\xi^+), \quad \xi^+ \geqslant 0, \\ f^R(t,0^-,\xi^-) = \alpha_R(\xi^-)f^R(t,0^-,-\xi^-), \quad \xi^- \leqslant 0, \end{cases} \tag{2.9}$$

$$\begin{cases} \mathcal{L}f^{T1} = 0, \quad f^{T1}(0,x,\xi) = f_0^{T1}(x,\xi) := I_{\{x<0\}}f_0(x,\xi), \\ f^{T1}(t,0^+,\xi^+) = \alpha_T(\xi^-)f^{T1}(t,0^-,\xi^-), \quad \xi^+ \geqslant 0, \\ f^{T1}(t,0^-,\xi^-) = \alpha_T(\xi^+)f^{T1}(t,0^+,\xi^+), \quad \xi^- \leqslant 0, \end{cases} \tag{2.10}$$

and

$$\begin{cases} \mathcal{L}f^{T2} = 0, \quad f^{T2}(0,x,\xi) = f_0^{T2}(x,\xi) := I_{\{x\geqslant 0\}}f_0(x,\xi), \\ f^{T2}(t,0^+,\xi^+) = \alpha_T(\xi^-)f^{T2}(t,0^-,\xi^-), \quad \xi^+ \geqslant 0, \\ f^{T2}(t,0^-,\xi^-) = \alpha_T(\xi^+)f^{T2}(t,0^+,\xi^+), \quad \xi^- \leqslant 0, \end{cases} \tag{2.11}$$

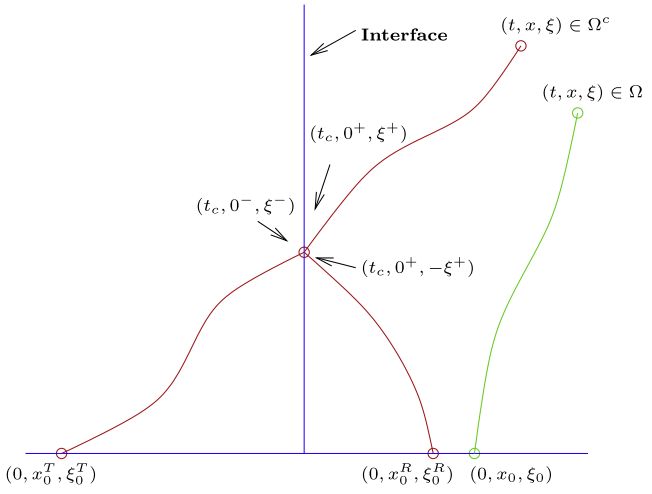

Fig. 1. Illustration of the characteristic solution.

where ξ^+ and ξ^- satisfy condition (2.6) with the same sign. If the characteristics of the Liouville equation, defined by (1.10), emanating from the support of $f_0(x,\xi)$ at time 0, intersect the interface at most once in the interval $[0,\tau_1]$ for some $\tau_1 > 0$. Then

$$f = f^R + I_{\{x\geqslant 0\}} f^{T1} + I_{\{x<0\}} f^{T2}, \quad 0 \leqslant t \leqslant \tau_1. \tag{2.12}$$

Proof. Let $0 \leqslant t \leqslant \tau_1$. We decompose the $x-\xi$ plane into two parts: $\Omega(t)$ and $\Omega^c(t)$. According to the definition of the solution to (2.5),

$$f(t,x,\xi) = I_\Omega f_0(x_0,\xi_0) + I_{\Omega^c}\alpha_R(\xi^+) f_0(x_0^R,\xi_0^R) + I_{\Omega^c}\alpha_T(\xi^-) f_0(x_0^T,\xi_0^T). \tag{2.13}$$

Similarly,

$$f^R(t,x,\xi) = I_\Omega f_0(x_0,\xi_0) + I_{\Omega^c}\alpha_R(\xi^+) f_0(x_0^R,\xi_0^R), \tag{2.14}$$

$$f^{T1}(t,x,\xi) = I_\Omega I_{\{x_0<0\}} f_0(x_0,\xi_0) + I_{\Omega^c}\alpha_T(\xi^-) I_{\{x_0^T<0\}} f_0(x_0^T,\xi_0^T), \tag{2.15}$$

$$f^{T2}(t,x,\xi) = I_\Omega I_{\{x_0\geqslant 0\}} f_0(x_0,\xi_0) + I_{\Omega^c}\alpha_T(\xi^-) I_{\{x_0^T\geqslant 0\}} f_0(x_0^T,\xi_0^T). \tag{2.16}$$

By the definitions of Ω, for all $(x,\xi)\in\Omega$, one can trace backward in time along the trajectory of (1.10) to (x_0,ξ_0) without hitting the interface $x = 0$. Therefore, $x_0 < 0$ if and only if $x < 0$. Thus

$$I_\Omega I_{\{x_0<0\}} = I_{\Omega\bigcap\{x<0\}}, \quad I_\Omega I_{\{x_0\geqslant 0\}} = I_{\Omega\bigcap\{x\geqslant 0\}}.$$

Similarly, definitions of Ω^c and x_0^T imply that

$$I_{\Omega^c} I_{\{x_0^T<0\}} = I_{\Omega^c\bigcap\{x\geqslant 0\}}, \quad I_{\Omega^c} I_{\{x_0^T\geqslant 0\}} = I_{\Omega^c\bigcap\{x<0\}}.$$

Hence

$$\begin{aligned} f^R(t,x,\xi) + I_{\{x\geqslant 0\}} f^{T1}(t,x,\xi) + I_{\{x<0\}} f^{T2}(t,x,\xi) &= I_\Omega f_0(x_0,\xi_0) + I_{\Omega^c}\alpha_R(\xi^+) f_0(x_0^R,\xi_0^R) + I_{\{x\geqslant 0\}} I_{\Omega\bigcap\{x<0\}} f_0(x_0,\xi_0) \\ &\quad + I_{\{x\geqslant 0\}} I_{\Omega^c\bigcap\{x\geqslant 0\}}\alpha_T(\xi^-) f_0(x_0^T,\xi_0^T) + I_{\{x<0\}} I_{\Omega\bigcap\{x\geqslant 0\}} f_0(x_0,\xi_0) \\ &\quad + I_{\{x<0\}} I_{\Omega^c\bigcap\{x<0\}}\alpha_T(\xi^-) f_0(x_0^T,\xi_0^T) \\ &= I_\Omega f_0(x_0,\xi_0) + I_{\Omega^c}\alpha_R(\xi^+) f_0(x_0^R,\xi_0^R) + I_{\Omega^c}\alpha_T(\xi^-) f_0(x_0^T,\xi_0^T) = f(t,x,\xi). \end{aligned}$$ □

Theorem 2.1 shows that an interface problem with partial transmissions and reflections can be decompose into the interface problems with complete transmissions and reflections, in a time interval in which the characteristics hit the interface at most once.

Based on this result, we can use the following strategy to obtain the solution of (2.5): for $0 \leqslant t \leqslant \tau_1$, we solve problems (2.9), (2.10) and (2.11), then

$$f(t,x,\xi) = f^R(t,x,\xi) + I_{\{x\geqslant 0\}} f^{T1}(t,x,\xi) + I_{\{x<0\}} f^{T2}(t,x,\xi), \quad 0 \leqslant t \leqslant \tau_1.$$

Using $f(\tau_1,x,\xi)$ as the initial data, we redo the previous step to get solution of (2.5) on $[\tau_1,\tau_1+\tau_2]$, where $\tau_2 > 0$ such that no particle trajectory will hit the interface more than once in the time period $[\tau_1,\tau_1+\tau_2]$. One can repeat this process to obtain the solution for any time interval $[0,K]$.

Remark 2.1. If there are N interfaces which divide $\mathbb{R}^1$ into $N+1$ parts denoted by $A_1, A_2, \ldots, A_{N+1}$, respectively, then the solution f will be

$$f = f^R + \sum_{i=1}^{N+1} I_{\{\mathbb{R}^1\setminus A_i\}} f^{T_i},$$

where each f^{T_i} has the initial data

$$f^{T_i}(0,x,\xi) = f_0^{T_i}(x,\xi) := I_{A_i} f_0(x,\xi).$$

Similarly, in the multi-dimensional case, if the interfaces divide $\mathbb{R}^d$ into $N+1$ parts denoted by $A_1, A_2, \ldots, A_{N+1}$, respectively, then the solution f will be

$$f = f^R + \sum_{i=1}^{N+1} I_{\{\mathbb{R}^d\setminus A_i\}} f^{T_i},$$

where each f^{T_i} has the initial data

$$f^{T_i}(0,\mathbf{x},\boldsymbol{\xi}) = f_0^{T_i}(\mathbf{x},\boldsymbol{\xi}) := I_{A_i} f_0(\mathbf{x},\boldsymbol{\xi}).$$

For general initial data or general geometry, it is not easy to determine $\tau_1, \tau_2, \ldots$ Here we propose a reinitialization after each time step Δt so f remains the form of (1.6). This will be addressed in Section 4.

3. The level set decomposition

Consider the δ function initial data (1.5), namely,

$$f(0,x,\xi) = f_0(x,\xi) = \rho_0(x)\delta(\xi - u_0(x)). \tag{3.1}$$

Correspondingly, the initial data for f^R, f^{T1} and f^{T2}, which only involve complete transmission or reflection, are of the mono-kinetic form (3.1). According to [14,15], they can be solved by the decomposition method of [9]. More specifically, $f^R = \psi^R\delta(\phi^R)$ where ϕ^R and ψ^R satisfy

$$\begin{cases} \mathcal{L}\phi^R = 0, \quad \phi_0^R(x) = \xi - u_0(x), \\ \phi^R(t,0^+,\xi^+) = \phi^R(t,0^+,-\xi^+), \quad \xi^+ \geqslant 0, \\ \phi^R(t,0^-,\xi^-) = \phi^R(t,0^-,-\xi^-), \quad \xi^- \leqslant 0, \end{cases} \tag{3.2}$$

$$\begin{cases} \mathcal{L}\psi^R = 0, \quad \psi_0^R(x) = \rho_0(x), \\ \psi^R(t,0^+,\xi^+) = \alpha_R(\xi^+)\psi^R(t,0^+,-\xi^+), \quad \xi^+ \geqslant 0, \\ \psi^R(t,0^-,\xi^-) = \alpha_R(\xi^-)\psi^R(t,0^-,-\xi^-), \quad \xi^- \leqslant 0, \end{cases} \tag{3.3}$$

Similarly, $f^{T1} = \psi^{T1}\delta(\phi^{T1})$ and $f^{T2} = \psi^{T2}\delta(\phi^{T2})$ where

$$\begin{cases} \mathcal{L}\phi^{T1} = 0, \quad \phi_0^{T1}(x) = \xi - u_0(x), \\ \phi^{T1}(t,0^+,\xi^+) = \phi^{T1}(t,0^-,\xi^-), \quad \xi^+ \geqslant 0, \\ \phi^{T1}(t,0^-,\xi^-) = \phi^{T1}(t,0^+,\xi^+), \quad \xi^- \leqslant 0, \end{cases} \tag{3.4}$$

$$\begin{cases} \mathcal{L}\psi^{T1} = 0, \quad \psi_0^{T1}(x) = I_{\{x<0\}}\rho_0(x), \\ \psi^{T1}(t,0^+,\xi^+) = \alpha_T(\xi^+)\psi^{T1}(t,0^-,\xi^-), \quad \xi^+ \geqslant 0, \\ \psi^{T1}(t,0^-,\xi^-) = \alpha_T(\xi^-)\psi^{T1}(t,0^+,\xi^+), \quad \xi^- \leqslant 0, \end{cases} \tag{3.5}$$

$$\begin{cases} \mathcal{L}\phi^{T2} = 0, \quad \phi_0^{T2}(x) = \xi - u_0(x), \\ \phi^{T2}(t,0^+,\xi^+) = \phi^{T2}(t,0^-,\xi^-), \quad \xi^+ \geqslant 0, \\ \phi^{T2}(t,0^-,\xi^-) = \phi^{T2}(t,0^+,\xi^+), \quad \xi^- \leqslant 0, \end{cases} \tag{3.6}$$

$$\begin{cases} \mathcal{L}\psi^{T2} = 0, \quad \psi_0^{T2}(x) = I_{\{x\geqslant 0\}}\rho_0(x), \\ \psi^{T2}(t,0^+,\xi^+) = \alpha_T(\xi^+)\psi^{T2}(t,0^-,\xi^-), \quad \xi^+ \geqslant 0, \\ \psi^{T2}(t,0^-,\xi^-) = \alpha_T(\xi^-)\psi^{T2}(t,0^+,\xi^+), \quad \xi^- \leqslant 0, \end{cases} \tag{3.7}$$

At time τ_1, one can sum these solutions to obtain

$$f(\tau_1) = f^R + I_{\{x\geqslant 0\}}f^{T1} + I_{\{x<0\}}f^{T2} = \psi^R\delta(\phi^R) + I_{\{x\geqslant 0\}}\psi^{T1}\delta(\phi^{T1}) + I_{\{x<0\}}\psi^{T2}\delta(\phi^{T2}). \tag{3.8}$$

4. Reinitialization

Clearly, in one space dimension, the maximal value of τ_1 depends on the distance between the discontinuities as well as the derivative of the potential in each smooth region. For general initial data and general piecewise smooth interfaces in higher space dimensions, it is not easy to determine τ_1. In this section we introduce a reinitialization procedure which can be carried out at each time step, after the decomposition step proposed in the previous section. With this decomposition–reinitialization process no knowledge of τ_1 is needed. When the discontinuity set of the potential is singular or the wave comes at critical angle, diffraction happens, which introduces a next order term and is out of the scope of this paper. We refer readers to [22,17,18].

As discussed in the previous section, even though f_0 has the form (3.1), at time τ_1 it is a sum of more than one delta functions. In fact, it may be the sum of more than three delta functions shown in (1.6), since ϕ^{R,T_1,T_2} may have multiple zeroes, corresponding to multiphased velocities [8,26]. Clearly, to continue the decomposition of Section 3, we need to reinitialize $f(\tau_1,x,\xi)$ so it becomes the form in (1.6). In other words, we want to find ϕ and ψ such that

$$\begin{aligned} f(x,\xi,\tau_1) &= \psi^R(x,\xi,\tau_1)\delta\big(\phi^R(x,\xi,\tau_1)\big) + I_{\{x\geqslant 0\}}\psi^{T1}(x,\xi,\tau_1)\delta\big(\phi^{T1}(x,\xi,\tau_1)\big) + I_{\{x<0\}}\psi^{T2}(x,\xi,\tau_1)\delta\big(\phi^{T2}(x,\xi,\tau_1)\big) \\ &= \psi(x,\xi,\tau_1)\delta(\phi(x,\xi,\tau_1)). \end{aligned} \tag{4.1}$$

The following theorems provide a generic strategy on how this can be done.

Theorem 4.1 (1-Dimension). *Assume $g_j(x)$ are continuous functions with N_j distinct zeros $x_{j_i}, i = 1,\ldots,N_j,\ j = 1,\ldots,N$. Assume $f_j(x)$ are bounded continuous functions. Then there exists an $\epsilon > 0$ and a function κ defined by*

$$\kappa(x) = \begin{cases} 1, & |x| < \epsilon, \\ 0, & |x| \geqslant \epsilon, \end{cases} \tag{4.2}$$

such that

$$\sum_{j=1}^{N} f_j(x)\delta(g_j(x)) = f(x)\delta(g(x)) \tag{4.3}$$

in the distributional sense. Here

$$f(x) = \sum_{j=1}^{N} f_j(x)\kappa(g_j(x)) \tag{4.4}$$

and $g(x)$ is defined by

$$g(x) = sgn(g_{l_x}(x)) \min_j(|g_j(x)|), \tag{4.5}$$

where l_x is the index such that $|g_{l_x}(x)| \leqslant |g_j(x)|,\ \forall\, j$.

Proof. Since $g_j(x)$ are continuous with distinct zeros, there exists an $\eta > 0$ small enough, such that

$$(x_{j_i} - \eta, x_{j_i} + \eta), \quad i = 1,\ldots,N_j,\ j = 1,\ldots,N$$

are disjoint intervals and

$$\max_{1\leqslant j\leqslant N, 1\leqslant i\leqslant N_j}\left(\max_{x\in(x_{j_i}-\eta,x_{j_i}+\eta)}|g_j(x)|\right) < \min_{1\leqslant j\leqslant N, 1\leqslant i\leqslant N_j}\left(\min_{x\in(x_{j_i}-\eta,x_{j_i}+\eta), m\neq j}|g_m(x)|\right),$$

Let

$$\epsilon = \max_{1\leqslant j\leqslant N, 1\leqslant i\leqslant N_j}\left(\max_{x\in(x_{j_i}-\eta,x_{j_i}+\eta)}(|g_j(x)|)\right), \tag{4.6}$$

then on each interval $(x_{j_i} - \eta, x_{j_i} + \eta)$,

$$f(x) = f_j(x)$$

and

$$g(x) = g_j(x).$$

Furthermore, one can find a positive number θ, such that

$$g(x) > \theta > 0, \quad \forall\, x \in \mathbb{R} \setminus \bigcup_{1\leqslant j\leqslant N, 1\leqslant i\leqslant N_j}(x_{j_i} - \eta, x_{j_i} + \eta). \tag{4.7}$$

Therefore, $\forall\ \varphi \in C_c^\infty(\mathbb{R})$,

$$\int_{-\infty}^{\infty}\varphi(x)f(x)\delta(g(x))dx = \sum_{j=1}^{N}\sum_{i=1}^{N_j}\int_{x_{j_i}-\eta}^{x_{j_i}+\eta}\varphi(x)f(x)\delta(g(x))dx. \tag{4.8}$$

Hence, for all test functions $\varphi \in C_c^\infty(\mathbb{R})$,

$$\begin{aligned}
&\int_{-\infty}^{\infty}\varphi(x)\sum_{j=1}^{N}f_j(x)\delta(g_j(x))dx \\
&= \sum_{j=1}^{N}\int\varphi(x)f_j(x)\delta(g_j(x))dx = \sum_{j=1}^{N}\sum_{i=1}^{N_j}\int_{x_{j_i}-\eta}^{x_{j_i}+\eta}\varphi(x)f_j(x)\delta(g_j(x))dx \\
&= \sum_{j=1}^{N}\sum_{i=1}^{N_j}\int_{x_{j_i}-\eta}^{x_{j_i}+\eta}\varphi(x)f(x)\delta(g(x))dx \\
&= \int_{-\infty}^{\infty}\varphi(x)f(x)\delta(g(x))dx.
\end{aligned} \tag{4.9}$$

This completes the proof. □

Theorem 4.2 (Multi-Dimension). *Assume $g_j(\mathbf{x})$ are C^1 continuous functions such that $\int_{\mathbb{R}^d}\delta(g_j(\mathbf{x}))d\mathbf{x}<\infty$ for $j=1,\ldots,N$. Denote the zeros sets of $g_j(\mathbf{x})$ by Ω_j. Assume that $\mathcal{M}(\Omega_{j_1}\cap\Omega_{j_2})=0,\ \forall\, j_1,j_2$. Suppose there exists a constant $C>0$ such that*

$$|Dg_j(\mathbf{x})|>C,\quad \forall\, j\quad \forall\,\mathbf{x}\in\Omega_j. \tag{4.10}$$

Let $f_j(\mathbf{x})$ be bounded continuous functions. Define the function κ_ϵ by

$$\kappa_\epsilon(\mathbf{x})=\begin{cases}1, & |\mathbf{x}|<\epsilon,\\ 0, & |\mathbf{x}|\geqslant\epsilon.\end{cases} \tag{4.11}$$

Then

$$f_\epsilon(\mathbf{x})\delta(g(\mathbf{x}))\rightharpoonup\sum_{j=1}^{N}f_j(\mathbf{x})\delta(g_j(\mathbf{x})),\quad \epsilon\to 0 \tag{4.12}$$

in the distributional sense. Here

$$f_\epsilon(\mathbf{x})=\sum_{j=1}^{N}f_j(\mathbf{x})\kappa_\epsilon(g_j(\mathbf{x})), \tag{4.13}$$

and $g(\mathbf{x})$ is defined by

$$g(\mathbf{x})=g_{k_{\mathbf{x}}}(\mathbf{x}), \tag{4.14}$$

where $k_{\mathbf{x}}$ is the index such that $|g_{k_{\mathbf{x}}}(\mathbf{x})|\leqslant|g_j(\mathbf{x})|,\forall\, j$.

Proof. For every fixed test function $\varphi(\mathbf{x})\in C_c^\infty(\mathbb{R}^d)$, for every fixed $\eta>0$, one can choose θ small enough such that

$$\left|\int_{\mathbb{R}^d}\varphi(\mathbf{x})\sum_{j=1}^{N}f_j(\mathbf{x})\delta(g_j(\mathbf{x}))d\mathbf{x}-\sum_{j=1}^{N}\int_{\Omega_j^\theta}\varphi(\mathbf{x})f_j(\mathbf{x})\delta(g_j(\mathbf{x}))d\mathbf{x}\right|<\frac{1}{2}\eta, \tag{4.15}$$

where Ω_j^θ is a subset of Ω_j with $\mathcal{M}(\Omega_j^\theta)<\infty$ and $\mathrm{dist}(\Omega_{j_1}^\theta,\Omega_{j_2}^\theta)>\theta>0,\ \forall\, j_1,j_2$. Following the same idea of the proof of Theorem 4.1, one can further choose a $\varrho>0$ small enough, such that if $0<\epsilon<\varrho$ then

$$\sum_{j=1}^{N}\int_{\Omega_j^\theta}\varphi(\mathbf{x})f_j(\mathbf{x})\delta(g_j(\mathbf{x}))d\mathbf{x}=\int_{\cup\Omega_j^\theta}\varphi(\mathbf{x})f_\epsilon(\mathbf{x})\delta(g(\mathbf{x}))d\mathbf{x}. \tag{4.16}$$

We chose $\theta>0$ small enough so that

$$\int_{\mathbb{R}^d\setminus\bigcup\Omega_j^\theta}\varphi(\mathbf{x})\left(\sum_{j=1}^{N}|f_j(\mathbf{x})|\right)\delta(g(\mathbf{x}))d\mathbf{x}<\frac{1}{2}\eta. \tag{4.17}$$

Combining (4.15), (4.16) and (4.17), we obtain that for every fixed $\varphi(\mathbf{x})\in C_c^\infty(\mathbb{R}^d)$, and for every fixed $\eta>0$, there exists $\varrho>0$, such that if $0<\epsilon<\varrho$, then

$$\left|\int_{\mathbb{R}^d}\varphi(\mathbf{x})\sum_{j=1}^{N}f_j(\mathbf{x})\delta(g_j(\mathbf{x}))d\mathbf{x}-\int_{\mathbb{R}^d}\varphi(\mathbf{x})f_\epsilon(\mathbf{x})\delta(g(\mathbf{x}))d\mathbf{x}\right|<\eta. \tag{4.18}$$

□

Corollary 4.1. *If $d\geqslant 2$ and $g_j(\mathbf{x})$ are piecewise C^1 continuous functions, then the conclusion of Theorem 4.2 is still true.*

Formally, the computational complexity of the reinitialization process (even it is performed after each time step) is the same as of solving (2.9), (2.10) and (2.11), which is also the same as solving the Liouville equation (2.5) directly. All of them have order $O(\Delta x^{-1}\Delta\xi^{-1})$. Furthermore, all of the functions $\phi^{R,T1,T2}$ and $\psi^{R,T1,T2}$ only need to be solved locally around the zero level sets of $\phi^{R,T1,T2}$. Therefore, the entire algorithm can be implemented using the local level set methods.

5. Numerical examples

In this section, we give several numerical examples. In each example, we compute the density and momentum which are given by

$$\rho=\int f(t,x,\xi)d\xi,$$
$$\rho u=\int \xi f(t,x,\xi)d\xi.$$

We use the upwind scheme to compute all the one-dimensional examples with a minmod slope limiter and the two-dimensional example with no slope limiter.

When computing the physical observables, we use the following discretized delta function [4],

$$\delta_b(x) = \begin{cases} \frac{1}{2b}(1+\cos\frac{|\pi x|}{b}), & |\frac{x}{b}| \leqslant 1, \\ 0, & \text{otherwise}, \end{cases} \tag{5.1}$$

where the parameter b is taken as $b = 0.5\sqrt{\Delta x}$.

Example 5.1 (*Plane waves*). We consider (2.5) with the following parameters:

$$V = \begin{cases} 0 & x \leqslant 0, \\ 0.045 & x > 0, \end{cases}$$

and the initial conditions:

$$f_0(x,\xi) = \rho_0(x)\delta(\xi - u_0(x)), \quad \rho_0(x) = I_{\{x\leqslant 0\}}, \quad u_0(x) = 0.5.$$

By the conservation of Hamiltonian,

$$\frac{0.5^2}{2} = 0.045 + \frac{(\xi^+)^2}{2},$$

one has $\xi^+ = 0.4$. Therefore,

$$\alpha_R = \frac{(\xi^- - \xi^+)^2}{(\xi^- + \xi^+)^2} = 0.012, \quad \alpha_T = \frac{4\xi^-\xi^+}{(\xi^- + \xi^+)^2} = 0.988. \tag{5.2}$$

One could solve this problem analytically, and the solution at the time $t = 1$ is

$$f(t,x,\xi) = I_{\{x\leqslant 0\}}\delta(\xi - 0.5) + 0.012 I_{\{-0.5\leqslant x\leqslant 0\}}\delta(\xi + 0.5) + 1.235 I_{\{0\leqslant x\leqslant 0.4\}}\delta(\xi - 0.4).$$

The analytical density and momentum are given by

$$\rho = \begin{cases} 1 & x \leqslant -0.5, \\ 1.012 & -0.5 < x \leqslant 0, \\ 1.235 & 0 < x \leqslant 0.4, \\ 0 & 0.4 < x. \end{cases} \quad \rho u = \begin{cases} 0.5 & x \leqslant -0.5, \\ 0.494 & -0.5 < x \leqslant 0, \\ 0.494 & 0 < x \leqslant 0.4, \\ 0 & 0.4 < x. \end{cases}$$

The errors and comparison figures are given in Table 1 and Fig. 2. The convergence orders for the density and momentum are 0.5199 and 0.5120.

As we may see from this example, sometimes even though the incident and transmitted angles are fairly large, the reflection coefficient is still too small to be noticeable; on the other hand, the choice of the coefficients makes no difference in testing the method, therefore to better illustrate the performance of this numerical method, we will use artificial α_R, α_T in the numerical examples thereafter.

Example 5.2 (*Harmonic oscillator*). We consider (2.5) with the following parameters:

$$V = \begin{cases} x^2/20 & x \leqslant 0, \\ x^2/20 + 0.045 & x > 0. \end{cases} \quad \alpha_R = 0.2, \ \alpha_T = 0.8$$

and the initial conditions:

$$f_0(x,\xi) = \rho_0(x)\delta(\xi - u_0(x)), \quad \rho_0(x) = \exp(-100(x+0.3)^2), \quad u_0(x) = 0.5.$$

The reference solution is computed in fine mesh and using small time steps. The comparison is given in Fig. 3.

Example 5.3 (*Reinitialization*). We consider (2.5) with the following parameters:

$$V = \begin{cases} 0 & x \leqslant 0, \\ 2x^2 + 0.045 & x > 0. \end{cases} \quad \alpha_R = 0.2, \ \alpha_T = 0.8$$

and the initial conditions:

Table 1
Example 5.1, the l^1 errors of the density and momentum.

Δx	0.02	0.01	0.005
$\|\rho_{err}\|_1$	8.55×10^{-2}	5.87×10^{-2}	4.16×10^{-2}
$\|(\rho u)_{err}\|_1$	3.38×10^{-2}	2.33×10^{-2}	1.66×10^{-2}

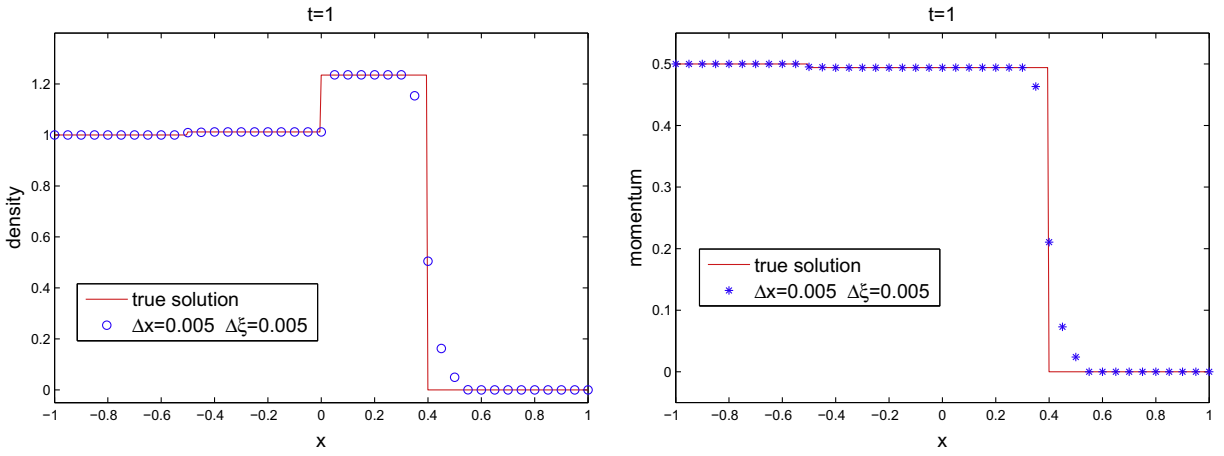

Fig. 2. Example 5.1, the comparison of density and momentum between the analytical solution and numerical solution.

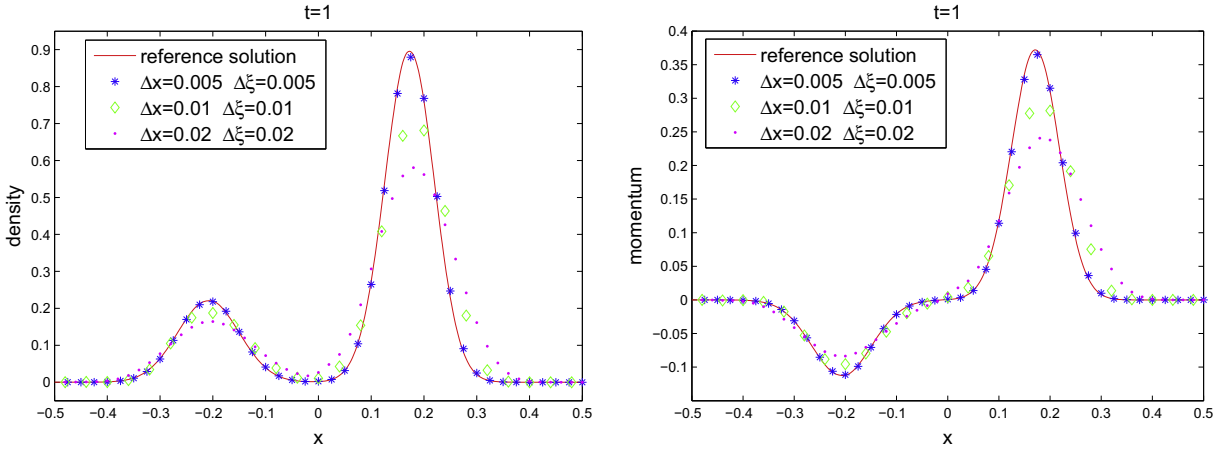

Fig. 3. Example 5.2, the comparison of density and momentum between the reference solution and numerical solution.

$$f_0(x,\xi) = \rho_0(x)\delta(\xi - u_0(x)), \quad \rho_0(x) = I_{\{x\leqslant 0\}}, \quad u_0(x) = 0.5.$$

In this example, the particles will hit the interface frequently due to the strong harmonic potential in the domain $\{x > 0\}$. We assume the speed of the particle becomes zero at $x = x_{turn}$, then by the conservation of Hamiltonian,

$$\frac{0.5^2}{2} = 0.045 + \frac{(\xi^+)^2}{2} = 0.045 + 4x_{turn}^2,$$

one has $\xi^+ = 0.4$, $x_{turn} = 0.2$, which implies a lower bound for the reinitialization time is $\tau_1 = 1$ (actually the second hitting time is $t = \pi/2$).

We compare the numerical solution with analytical solution at $t = 1$ and $t = 2$. When reinitialization, we let κ be the following cutoff function

$$\kappa(x) = \begin{cases} 1, & |x| \leqslant 0.5\sqrt{\Delta x}, \\ 0, & |x| > 0.5\sqrt{\Delta x}. \end{cases}$$

Following [27], one can find the analytical solution. The analytical solution at $t = 1$ is given by

$$f(1,x,\xi) = I_{\{x\leqslant 0\}}\delta(\xi - 0.5) + 0.2I_{\{-0.5\leqslant x\leqslant 0\}}\delta(\xi + 0.5) + 0.8I_{\{0\leqslant x\leqslant 0.2\}}\frac{1}{0.8\sqrt{1-25x^2}}\delta\left(\xi - 0.4\sqrt{1-25x^2}\right) + 0.8I_{\{0.2\sin 2\leqslant x<0.2\}}\frac{1}{0.8\sqrt{1-25x^2}}\delta\left(\xi + 0.4\sqrt{1-25x^2}\right). \tag{5.3}$$

The analytical density and momentum at $t = 1$ are given by

$$\rho = \begin{cases} 1 & x \leqslant -0.5, \\ 1.2 & -0.5 < x \leqslant 0, \\ \frac{1}{\sqrt{1-25x^2}} & 0 < x \leqslant 0.2\sin 2, \\ \frac{2}{\sqrt{1-25x^2}} & 0.2\sin 2 < x \leqslant 0.2, \\ 0 & x > 0.2. \end{cases} \qquad \rho u = \begin{cases} 0.5 & x \leqslant -0.5, \\ 0.4 & -0.5 < x \leqslant 0, \\ 0.4 & 0 < x \leqslant 0.2\sin 2, \\ 0 & 0.2\sin 2 < x. \end{cases}$$

The analytical solution at $t = 2$ is given by

$$\begin{aligned} f(2,x,\xi) &= I_{\{x\leqslant 0\}}\delta(\xi-0.5) + 0.2I_{\{-1\leqslant x\leqslant 0\}}\delta(\xi+0.5) + 0.64I_{\{\pi/4-1\leqslant x<0\}}\delta(\xi+0.5) + 0.8I_{\{0\leqslant x\leqslant 0.2\}} \\ &\quad\times \frac{1}{0.8\sqrt{1-25x^2}}\delta\left(\xi - 0.4\sqrt{1-25x^2}\right) + 0.8I_{\{0\leqslant x<0.2\}}\frac{1}{0.8\sqrt{1-25x^2}}\delta\left(\xi+0.4\sqrt{1-25x^2}\right) \\ &\quad + 0.16I_{\{0\leqslant x\leqslant 0.2\sin 2(2-\pi/2)\}}\frac{1}{0.8\sqrt{1-25x^2}}\delta\left(\xi-0.4\sqrt{1-25x^2}\right). \end{aligned} \tag{5.4}$$

The analytical density and momentum at $t = 2$ are given by

$$\rho = \begin{cases} 1 & x \leqslant -1, \\ 1.2 & -1 < x \leqslant \pi/4-1, \\ 1.84 & \pi/4-1 < x \leqslant 0, \\ \frac{2.2}{\sqrt{1-25x^2}} & 0 < x \leqslant 0.2\sin 2(2-\pi/2), \\ \frac{2}{\sqrt{1-25x^2}} & 0.2\sin 2(2-\pi/2) < x \leqslant 0.2, \\ 0 & x > 0.2. \end{cases} \qquad \rho u = \begin{cases} 0.5 & x \leqslant -1, \\ 0.4 & -1 < x \leqslant \pi/4-1, \\ 0.08 & \pi/4-4 < x \leqslant 0, \\ 0.08 & 0 < x \leqslant 0.2\sin 2(2-\pi/2), \\ 0 & 0.2\sin 2(2-\pi/2) < x. \end{cases}$$

Since the density blows up at $x = 0.2$, we apply the following formula to calculate $f(2,x,\xi)$ and then the physical observables

$$f(2,x,\xi) = (\psi^R - I_{\{x\geqslant 0\}}\psi^{T2})\delta(\phi^R) + I_{\{x\geqslant 0\}}\psi^{T1}\delta(\phi^{T1}) + \psi^{T2}\delta(\phi^{T2}). \tag{5.5}$$

This formula is equivalent to (3.8). The advantage of (5.5) is that it singles out the pure reflection part and thus decreases the effect of the very large ρ on the momentum near 0.2. The comparison of the numerical solution and the analytical solution is given in Figs. 4–6.

We now compare with the direct method, in which one discretizes the δ function initial data and solves the Liouville equation directly. Using the same discretized delta function (5.1) with the same parameter $b = 0.5\sqrt{\Delta x}$, we compute the solution of this example by the direct method. The comparison of the results at time $t = 1$ and $t = 2$ is given in Figs. 7 and 8, which shows that the decomposition method proposed in this paper gives a much more accurate solution especially for longer time.

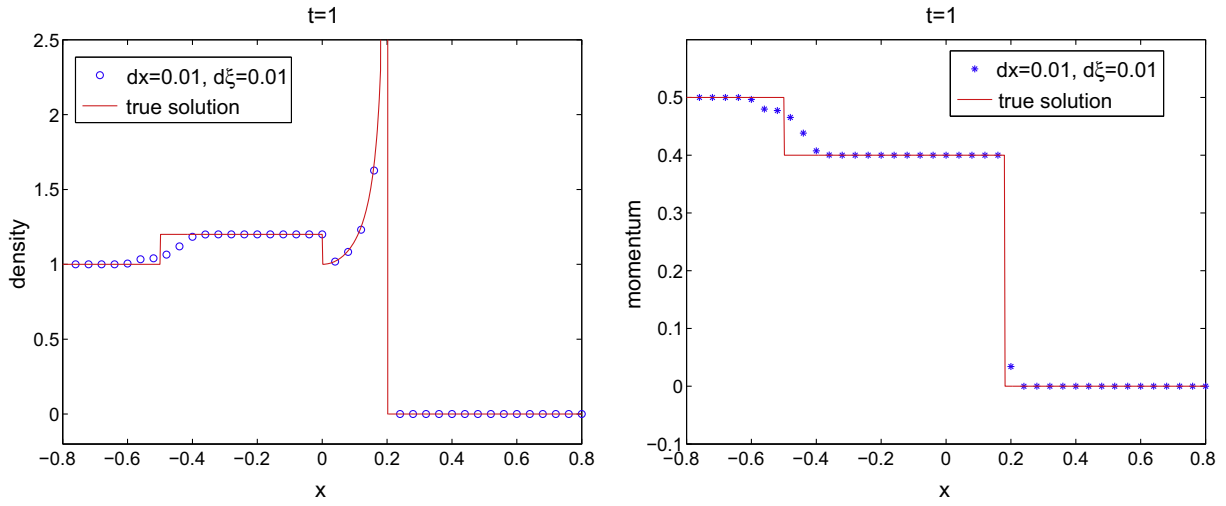

Fig. 4. Example 5.3, the comparison of density and momentum between the reference solution and numerical solution at $t = 1$.

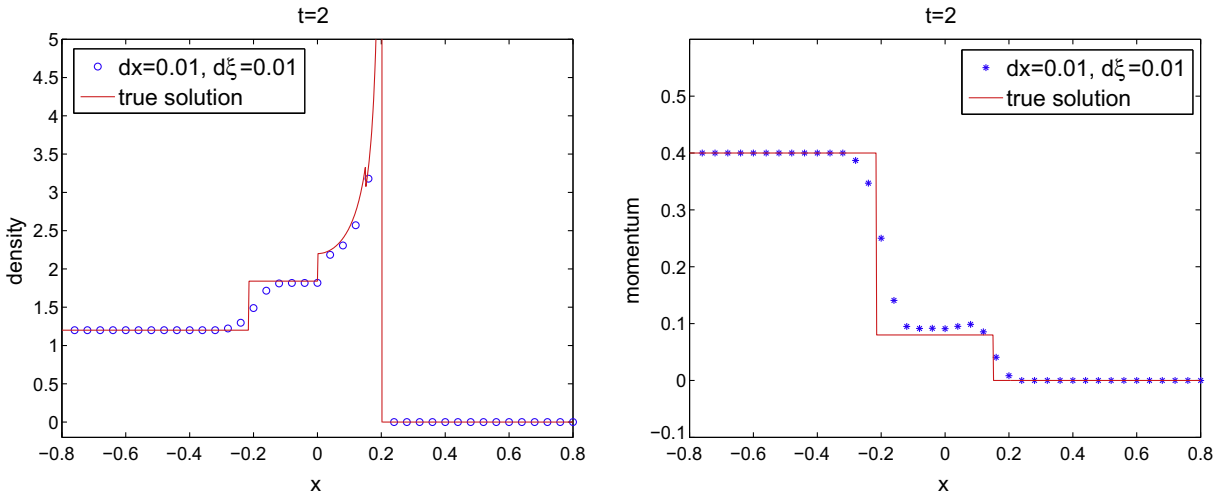

Fig. 5. Example 5.3, the comparison of density and momentum between the reference solution and numerical solution at $t = 2$, reinitialization was performed at $t = 1$.

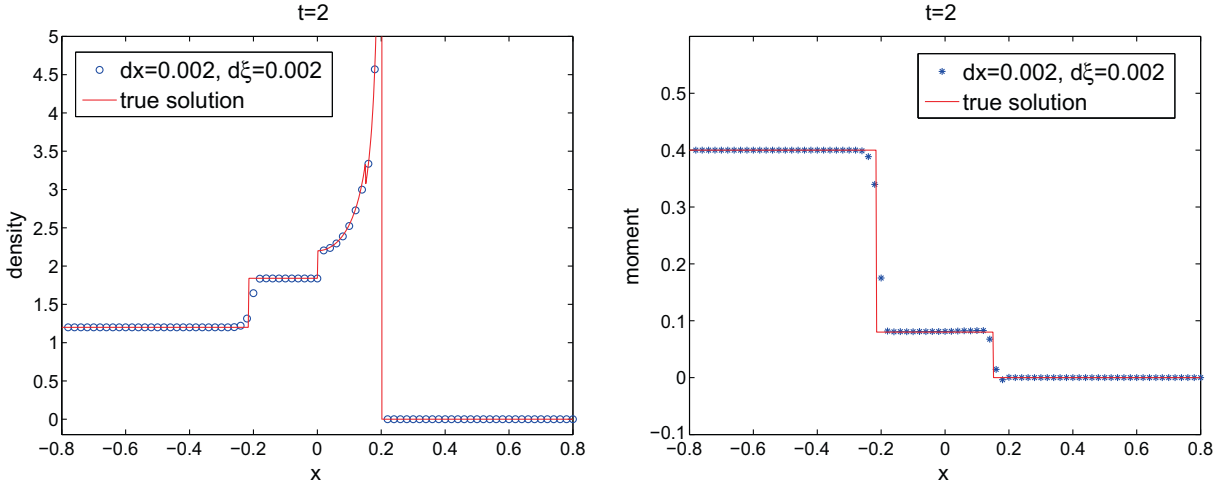

Fig. 6. Example 5.3, the comparison of density and momentum between the reference solution and numerical solution at $t = 2$ with a finer grid and $b = 0.15\sqrt{\Delta x}$, reinitialization was performed at $t = 1$.

Example 5.4 (*2d example*). We consider a two-dimensional interface problem in the domain $[-1,1] \times [-1,1]$. The potential well is given by

$$V = \begin{cases} 0 & (x,y) \in \Omega, \\ 1 & (x,y) \in \Omega^c. \end{cases} \quad \alpha_R = 0.2, \quad \alpha_T = 0.8,$$

where $\Omega = \{(x,y) | y > -0.4,\ y - x - 0.5 < 0,\ y + x - 0.5 < 0\}$. The initial condition is

$$f_0(\mathbf{x},\xi) = \rho_0(\mathbf{x})\delta(\xi - \mathbf{u}_0(\mathbf{x})), \quad \rho_0(\mathbf{x}) = \rho_0(x,y) = I_{\{|x+0.5|<0.05,\ y>0.2\}}, \quad \mathbf{u}_0 = (0,-\sqrt{2}).$$

See Fig. 9 for the illustration of the interface and the initial data.

We compare the numerical solution with analytical solution at $t = 1$. The analytical solution of the density at $t = 1$ can be obtained by the method of generalized characteristics, and it takes the following form:

$$\begin{aligned} \rho(x,y) = {} & I_{\text{reg1}}\delta(u - (0,-\sqrt{2})) + 0.2 I_{\text{reg2}}\delta(u - (-\sqrt{2},0)) + \frac{0.8}{\sqrt{3}} I_{\text{reg3}}\delta(u - (2\sin(\pi/12), -2\cos\pi/12)) \\ & + \frac{0.16}{\sqrt{3}} I_{\text{reg4}}\delta(u - (2\sin(\pi/12), 2\cos\pi/12)) + \frac{1.28\cos(\pi/12)}{\sqrt{12\cos^2(\pi/12) - 6}} I_{\text{reg5}}\delta(u - (2\sin(\pi/12), \\ & - \sqrt{4\cos^2(\pi/12) - 2}), \end{aligned}$$

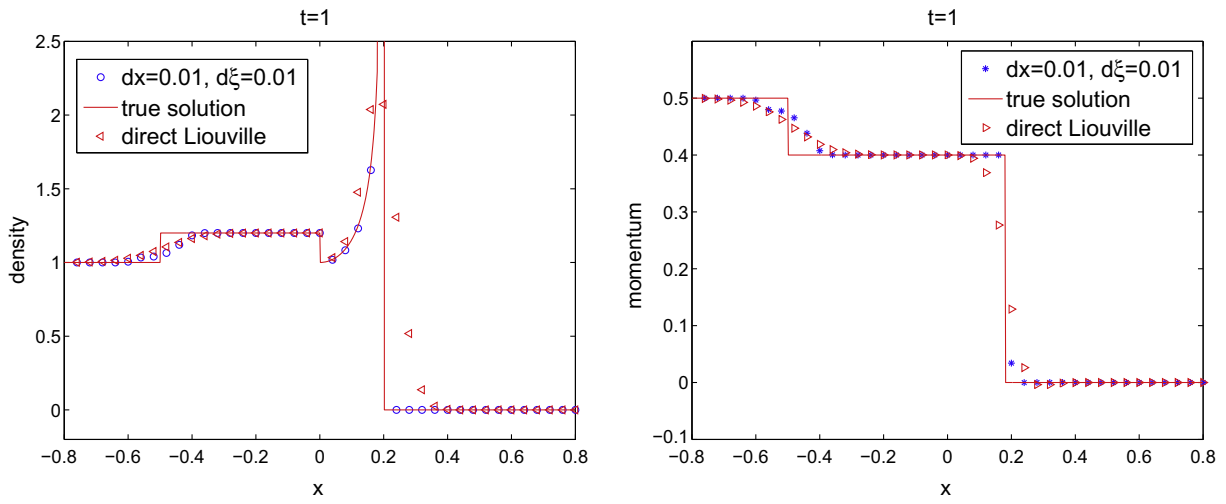

Fig. 7. Example 5.3, the comparison of density and momentum between the solutions obtained by our method and by the direct method.

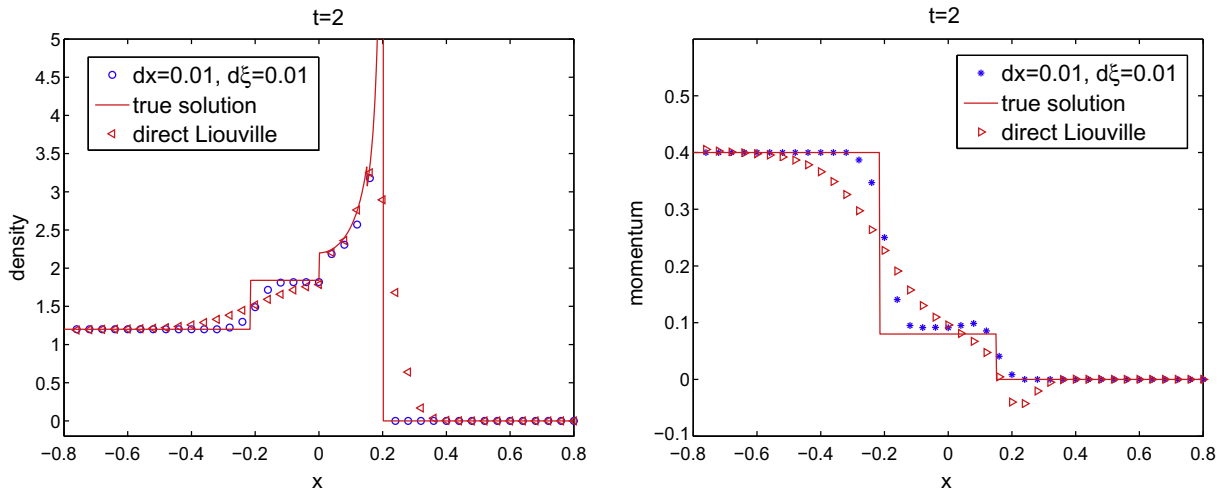

Fig. 8. Example 5.3, the comparison of density and momentum between the solutions obtained by our method and by the direct method.

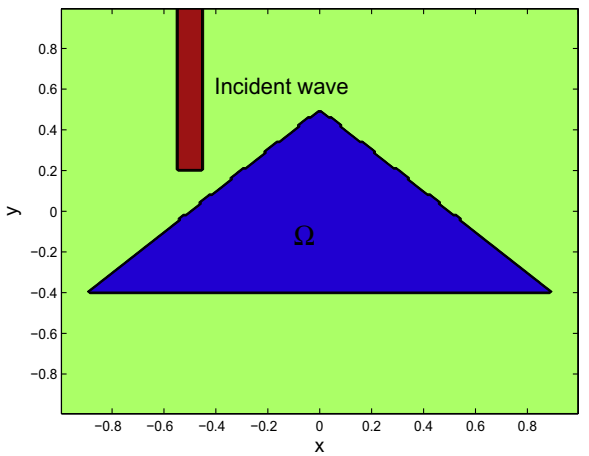

Fig. 9. Illustration of the potential well and initial conditions in Example 5.4.

where

$$\text{reg1} = \{(x,y)|\ y - x - 0.5 > 0,\ -0.55 < x < -0.45.\},$$
$$\text{reg2} = \{(x,y)|\ y - x - 0.5 > 0,\ -0.05 < y < 0.05.\},$$

$$\text{reg3} = \{(x,y)|\ y - x - 0.5 < 0,\ y > -0.4,\ y < 0.05 - (x + 0.45)/\tan(\pi/12),\ y > -0.05 - (x + 0.55)/\tan(\pi/12)\},$$

$$\text{reg4} = \{(x,y)|\ y - x - 0.5 < 0,\ y > -0.4,\ y > -0.4 + (x - x_1)/\tan(\pi/12),\ y < -0.4 + (x - x_2)/\tan(\pi/12)\},$$

$$\text{reg5} = \left\{(x,y)|\ y - x - 0.5 < 0,\ y < -0.4,\ y < -0.4 - (x - x_1)\frac{\sqrt{4\cos^2(\pi/12) - 2}}{2\sin(\pi/12)},\right.$$
$$\left. y > -0.4 - (x - x_2)\frac{\sqrt{4\cos^2(\pi/12) - 2}}{2\sin(\pi/12)}\right\},$$

$$x_1 = 0.45\tan(\pi/12) - 0.45, \quad x2 = 0.35\tan(\pi/12) - 0.55.$$

The comparison of the numerical solution and the exact solution was shown in Fig. 10, where the densities after the third transmission and reflection are ignored since their magnitudes are already very small. The absolute value of the difference between the numerical solution and exact solution was shown in Fig. 11. The mesh size is $\Delta x = 0.000625, \Delta y = 0.000625$ and the time step is taken to be $\Delta t = 0.000125$. In Table 2, the l^1 errors are given for different $\Delta x = \Delta y$. The convergence order is 0.5064.

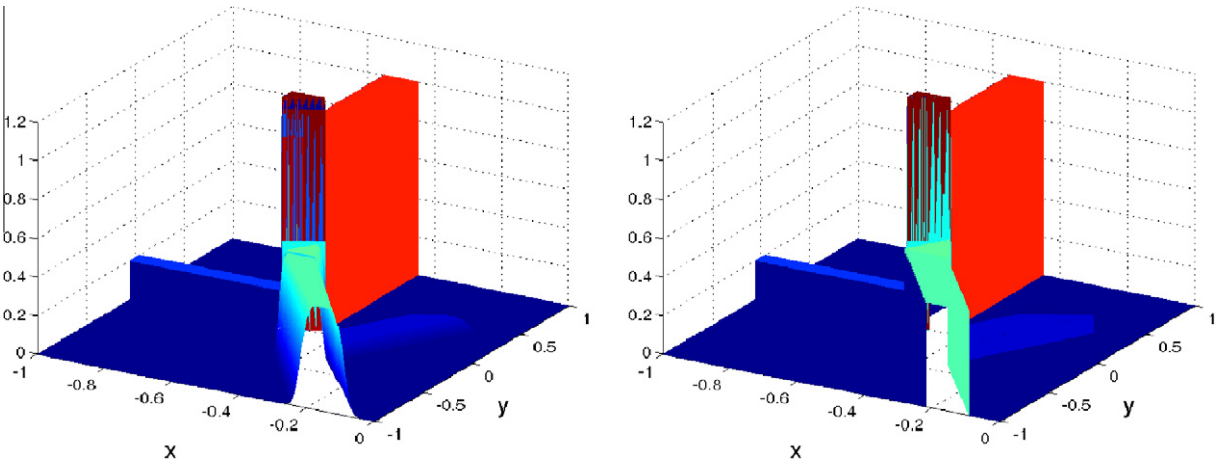

Fig. 10. Example 5.4, the comparison of density between the numerical solution (left) and true solution (right) at $t = 1$.

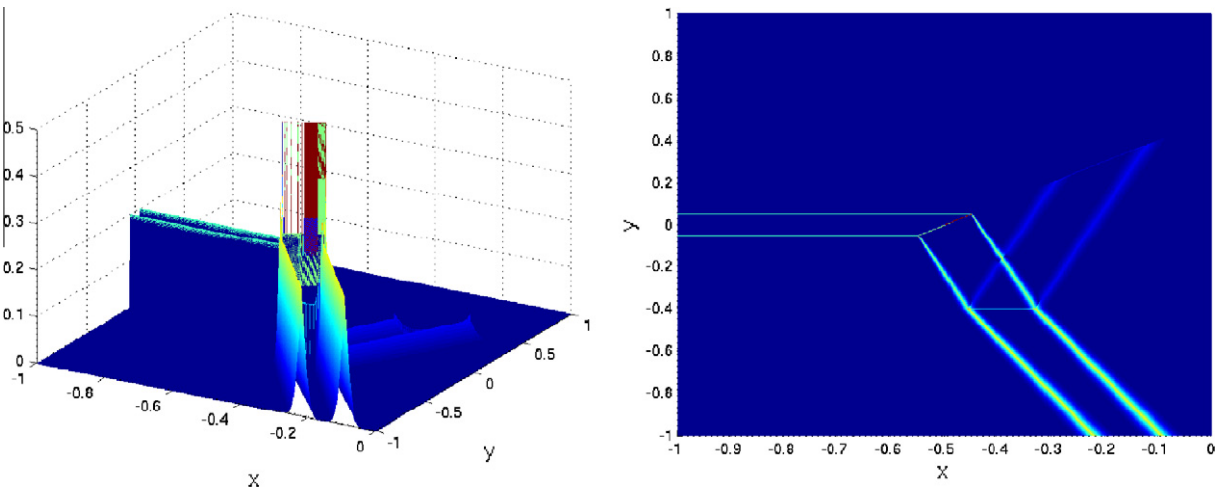

Fig. 11. Example 5.4, the difference between the numerical solution and true solution at t = 1 (left), a bird's eye view of the difference (right).

Table 2
Example 5.4, the l^1 errors of the density.

$\Delta x = \Delta y$	0.0025	0.00125	0.000625
$\|\rho_{err}\|_1$	1.128×10^{-1}	7.92×10^{-2}	5.59×10^{-2}

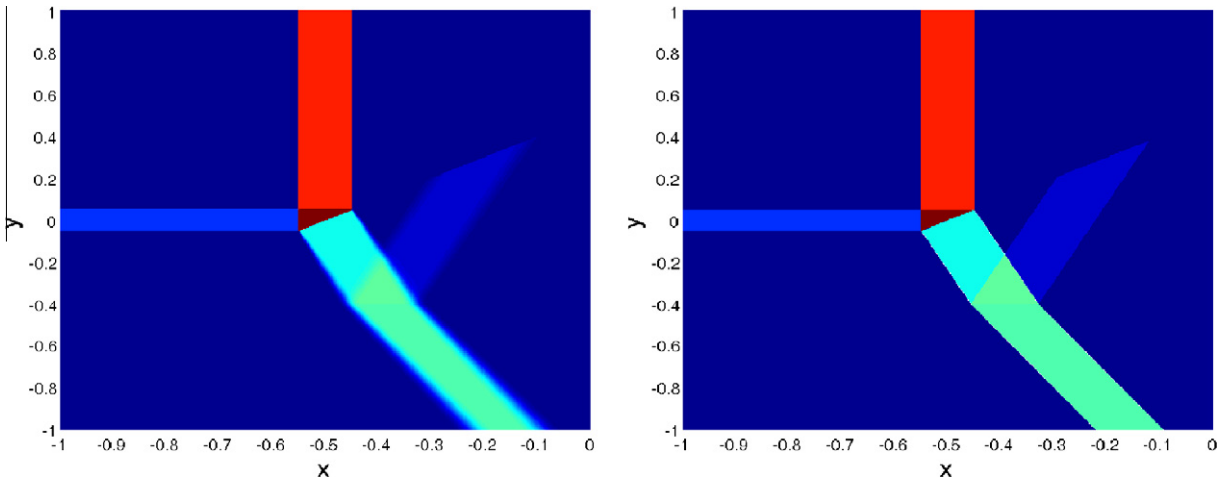

Fig. 12. Example 5.4, a bird's eye view of the density. Left: numerical solution. Right: true solution.

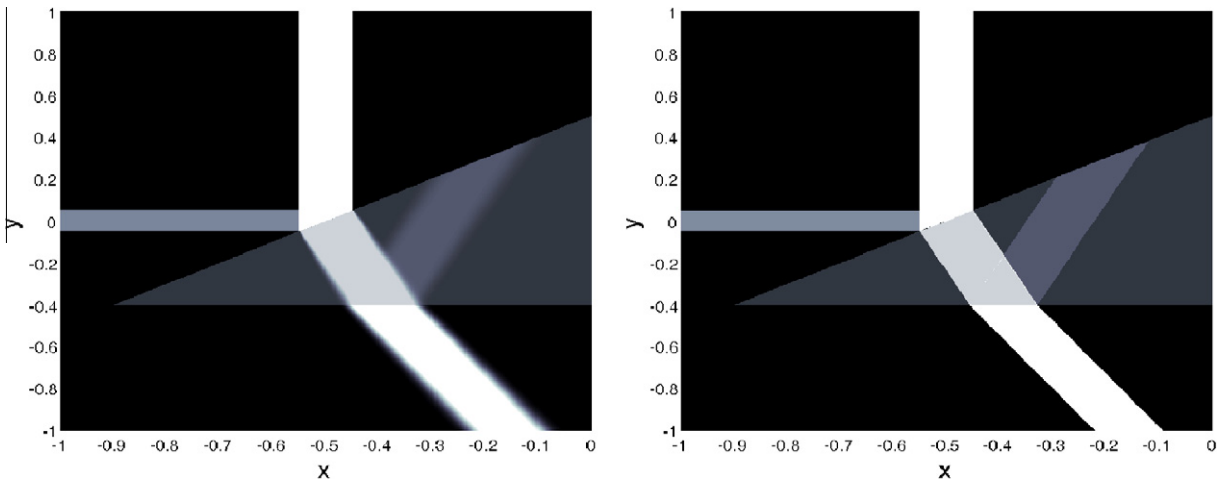

Fig. 13. Example 5.4, a bird's eye view of the density with interface plotted, to better illustrate the result, density was taken to be 2.5 times the original one. Left: numerical solution. Right: true solution.

Fig. 12 gives a bird's eye view of the solution.

Fig. 13 gives a bird's eye view of the solution with interface plotted. To better illustrate the result, the density in Fig. 13 was taken to be *2.5* times the original one.

6. Concluding remarks

In this paper, we proposed a level set method for the semiclassical limit of the Schrödinger equation with discontinuous potentials that correspond to potential barriers. At a potential barrier, waves can be partially transmitted and reflected. We combine the method of Jin–Wen [14,16]–using an interface condition for the Liouville equation to account for partial transmissions and reflections, and the level set decomposition method of [9], in order to have a level set method for partial transmissions and reflections with a higher numerical accuracy. We introduced two new ideas here. First, we decompose the solutions involving partial transmissions and reflections into a finite sum of solutions solving problems involving only complete transmissions and those involving only complete reflections, since for problems involving only complete transmission or complete reflection, the method of [9] can be applied for a higher numerical accuracy. This decomposition is only valid

when waves or particles hit the interface at most once. For more general problems, a reinitialization technique is introduced so that waves coming from multiple transmissions and reflections can be combined seamlessly as new initial value problems. This is implemented by rewriting the sum of several delta functions as one delta function with a suitable weight, which can be easily implemented numerically. Both one and two space dimension problems were used to demonstrate the validity of this new numerical method. One can extend the method to higher order accuracy by combining the technique proposed here and high order methods for computing physical observables, e.g., [28].

Acknowledgment

This work was partially supported by NSF Grant No. DMS-0608720, and NSF FRG grant DMS-0757285. SJ was also supported by a Van Vleck Distinguished Research Prize from University of Wisconsin-Madison. RT is partially supported by NSF DMS-0714612 and DMS-0914840, and an Alfred Sloan Foundation Fellowship.

References

[1] G. Bal, J.B. Keller, G. Papanicolaou, L. Ryzhik, Transport theory for acoustic waves with reflection and transmission at interfaces, Wave Motion 30 (1999) 303–327.
[2] Li-Tien Cheng, Myungjoo Kang, Stanley Osher, Hyeseon Shim, Yen-Hsi Tsai, Reflection in a level set framework for geometric optics, Comput. Model. Eng. Sci. 5 (2004) 347–360.
[3] L.-T. Cheng, H.-L. Liu, S. Osher, Computational high-frequency wave propagation using the level set method, with applications to the semi-classical limit of Schrödinger equations, Comm. Math. Sci. 1 (2003) 593–621.
[4] B. Engquist, A.K. Tornberg, R. Tsai, Discretization of Dirac delta functions in level set methods, J. Comput. Phys. 207 (1) (2005) 28–51.
[5] B. Engquist, O. Runborg, A.-K. Tornberg, High-frequency wave propagation by the segment projection method, J. Comput. Phys. 178 (2) (2002) 373–390.
[6] P. Gerard, P.A. Markowich, N.J. Mauser, F. Poupaud, Homogenization limits and Wigner transforms, Comm. Pure Appl. Math. 50 (4) (1997) 323–379.
[7] S. Jin, Numerical methods for hyperbolic systems with singular coefficients: well-balanced scheme, Hamiltonian preservation, and beyond, in: Proceedings of the 12th International Conference on Hyperbolic Problems: Theory, Numerics, Applications, University of Maryland, College Park. Proceedings of Symposia in Applied Mathematics, vol. 67-1, American Mathematical Society, 2009, pp. 93–104.
[8] S. Jin, X.T. Li, Multi-phase computations of the semiclassical limit of the Schrodinger equation and related problems: Whitham vs. Wigner, Physica D 182 (2003) 46–85.
[9] S. Jin, H.L. Liu, S. Osher, R. Tsai, Computing multivalued physical observables for the semiclassical limit of the Schrodinger equation, J. Comp. Phys. 205 (2005) 222–241.
[10] S. Jin, K. Novak, A semiclassical transport model for thin quantum barriers, Multiscale Model. Simul. 5 (4) (2006) 1063–1086.
[11] S. Jin, K. Novak, A semiclassical transport model for two-dimensional thin quantum barriers, J. Comp. Phys. 226 (2007) 1623–1644.
[12] S. Jin, K. Novak, A coherent semiclassical transport model for pure-state quantum scattering, Comm. Math. Sci. 8 (2010) 253–275.
[13] S. Jin, S. Osher, A level set method for the computation of multi-valued solutions to quasi-linear hyperbolic PDE's and Hamilton–Jacobi equations, Comm. Math. Sci. 1 (3) (2003) 575–591.
[14] S. Jin, X. Wen, Hamiltonian-preserving schemes for the Liouville equation with discontinuous potentials, Comm. Math. Sci. 3 (2005) 285–315.
[15] S. Jin, X. Wen, Hamiltonian-preserving schemes for the Liouville equation of geometrical optics with discontinuous local wave speeds, J. Comp. Phys. 214 (2006) 672–697.
[16] S. Jin, X. Wen, Hamiltonian-preserving schemes for the Liouville equation of geometrical optics with partial transmissions and reflections, SIAM J. Num. Anal. 44 (2006) 1801–1828.
[17] S. Jin, D. Yin, Computational high frequency waves through curved interfaces via the Liouville equation and Geometric Theory of Diffraction, J. Comp. Phys. 227 (2008) 6106–6139.
[18] S. Jin, D. Yin, Computation of high frequency wave diffraction by a half plane via the Liouville equation and Geometric Theory of Diffraction, Comm. Comput. Phys. 4 (5) (2008) 1106–1128.
[19] S.Y. Leung, J. Qian, S.J. Osher, A level set method for three-dimensional paraxial geometrical optics with multiple sources, Commun. Math. Sci. 2 (2004) 643–672.
[20] P.L. Lions, T. Paul, Sur les measures de Wigner, Revista. Mat. Iberoamericana 9 (1993) 553–618.
[21] L. Miller, Refraction of high frequency waves density by sharp interfaces and semiclassical measures at the boundary, J. Math. Pures Appl. IX 79 (2000) 227–269.
[22] M. Motamed, O. Runborg, A multiple-patch phase space method for computing trajectories on manifolds with applications to wave propagation problems, Comm. Math. Sci. 5 (2007) 617–648.
[23] S. Osher, L.-T. Cheng, M. Kang, H. Shim, Y.-H. Tsai, Geometric optics in a phase-space-based level set and Eulerian framework, J. Comput. Phys. 179 (2) (2002) 622–648.
[24] J. Qian, S.Y. Leung, A level set method for multivalued solutions of paraxial eikonal equations, J. Comput. Phys. 197 (2004) 711–736.
[25] L. Ryzhik, G. Papanicolaou, J. Keller, Transport equations for waves in a half space, Comm. PDE's 22 (1997) 1869–1910.
[26] C. Sparber, P. Markowich, N. Mauser, Multivalued geometrical optics: Wigner vs. WKB, Asymptotic Anal. 33 (2003) 1530187.
[27] D. Wei, Weak solutions of the one-component and two-component 1D Vlasov–Poisson equations with electron sheet initial data, preprint.
[28] X. Wen, A high order numerical method for computing physical observables in the semiclassical limit of the one dimensional linear Schrödinger equation with discontinuous potentials, J. Sci. Comput. 42 (2) (2010) 318–344.